Research Article | Vol. 31, No. 19 / 11 Sep 2023 / Optics Express 30723
Optics EXPRESS

Efficient capacity enhancement using OFDM with interleaved subcarrier number modulation in bandlimited UOWC systems

JIAMIN CHEN,[1,†] BOHUA DENG,[2,†] CHEN CHEN,[1,4] MIN LIU,[1] H. Y. FU,[2,5] AND HARALD HAAS[3]

[1]School of Microelectronics and Communication Engineering, Chongqing University, Chongqing 400044, China
[2]Tsinghua Shenzhen International Graduate School, Tsinghua University, Shenzhen 518055, China
[3]Technology Innovation Centre and Department of Electronic and Electrical Engineering, University of Strathclyde, G1 1RD Glasgow, UK
[4]c.chen@cqu.edu.cn
[5]hyfu@sz.tsinghua.edu.cn
[†]These authors contributed equally to this work

Abstract: We propose and demonstrate an efficient capacity enhancement scheme for bandlimited underwater optical wireless communication (UOWC) systems by utilizing orthogonal frequency division multiplexing with interleaved subcarrier number modulation (OFDM-ISNM). In the proposed OFDM-ISNM, joint number and constellation mapping/de-mapping is utilized to avoid error propagation and subblock interleaving is further applied to address the low-pass effect of the bandlimited UOWC system. The feasibility and superiority of the proposed OFDM-ISNM scheme for practical bandlimited UOWC systems have been verified through both simulations and experiments. The obtained results demonstrate that the proposed OFDM-ISNM scheme is capable of efficiently improving the achievable data rate of the bandlimited UOWC system. Specifically, the experimental results show a significant 28.6% capacity enhancement by OFDM-ISNM over other benchmark schemes, achieving a data rate of 3.6 Gbps through a 2-m water channel.

1. Introduction

In recent years, optical wireless communication (OWC) has been widely recognized as an efficient technology for communication in underwater environments [1,2]. Compared with traditional underwater wireless communication technologies such as underwater acoustic communication and underwater radio frequency communication, underwater OWC (UOWC) has many distinct advantages including huge spectrum resources, low transmission latency, high physical-layer security, small size and low cost [3,4]. Despite all these advantages, practical UOWC systems are generally bandlimited and exhibit a typical low-pass characteristic, due to the low-pass nature of the adopted components such as light-emitting diodes (LEDs), laser diodes (LDs) and photo-detectors (PDs) [5]. As a result, the usable bandwidth of practical bandlimited UOWC systems might not be sufficient enough to fully explore the potential of the system to achieve high-speed data transmission.

To address the bandwidth limitation issue of practical bandlimited UOWC systems, many techniques have been reported in the literature. On the one hand, the usable bandwidth of bandlimited UOWC systems can be directly extended via various pre- or post-equalization schemes [6–9]. Nevertheless, the feedback of channel information is generally required to successfully perform pre-equalization which inevitably increases the training overhead and the implementation complexity of the system, and meanwhile pre-equalization might also be vulnerable to LED/LD nonlinearity when the low-pass effect is relatively severe [10]. Moreover, the computational complexity of post-equalization is usually high which might limit its application

#496965 https://doi.org/10.1364/OE.496965
Journal © 2023 Received 1 Jun 2023; revised 23 Aug 2023; accepted 23 Aug 2023; published 1 Sep 2023

Optics EXPRESS

in many practical scenarios. On the other hand, the achievable data rate can be improved by increasing the number of bits that can be transmitted per unit bandwidth, i.e., spectral efficiency. Particularly, spectral-efficient modulation techniques such as orthogonal frequency division multiplexing (OFDM) has been widely applied to enhance the spectral efficiency of bandlimited UOWC systems [11–14]. Moreover, OFDM with bit and power loading has been reported to further improve the spectral efficiency of bandlimited UOWC systems [15]. Nevertheless, the implementation complexity and cost of OFDM with bit and power loading can be much higher than that of plain OFDM, which might limit its practical application in resource-limited underwater environments [16]. Besides OFDM, OFDM with subcarrier index modulation (OFDM-SIM) has also been introduced for both free-space and underwater OWC systems, which can achieve improved bit error rate (BER) performance than plain OFDM [17–20]. For both OFDM and OFDM-SIM, the high-frequency subcarriers inevitably suffer from a high power attenuation due to the low-pass frequency response of the bandlimited UOWC system. Lately, OFDM with subcarrier number modulation (OFDM-SNM) has been proposed to further enhance the performance of OFDM, which changes the number of activated subcarriers to convey additional information bits [21,22]. However, OFDM-SNM has not yet been considered in bandlimited UOWC systems and whether it can bring benefits to mitigate the adverse low-pass effect of the bandlimited UOWC systems is still an open question.

In this paper, we for the first time propose and demonstrate an efficient capacity enhancement scheme for bandlimited UOWC systems by using OFDM with interleaved subcarrier number modulation (OFDM-ISNM). By performing subblock interleaving, OFDM-ISNM can concentrate the activated subcarriers in the low-frequency region and hence mitigate the adverse low-pass effect. Both simulations and experiments have been conducted to evaluate and compare the performance of a bandlimited UOWC system applying OFDM-ISNM and other benchmark schemes.

2. Principle

2.1. OFDM-ISNM

Figures 1(a) and 1(b) illustrate the schematic diagrams of OFDM-ISNM transmitter and receiver, respectively. For the transmission of each OFDM block, a total of m information bits enter the OFDM-ISNM transmitter. These m bits are first split into G groups each obtaining b bits, i.e., $m = bG$. Each group of b bits is mapped to an OFDM subblock of length n , where $n = N/G$, and N is the number of data subcarriers. In each subblock, joint number and constellation mapping is utilized to avoid error propagation. Let $K = \{k_1, \ldots, k_l\}$ represent the adopted number set of the activated subcarriers with size l, where k_i denotes a specific number of the activated subcarriers with $i = 1, \ldots, l$ and $k_i \in \{0, \ldots, n\}$. Hence, K is a subset of $\{0, \ldots, n\}$ and the corresponding number of information bits that can be transmitted in each subblock can be obtained by

$$b = \lfloor \log_2(M^{k_1} + M^{k_2} + \cdots + M^{k_l}) \rfloor, \tag{1}$$

where M is the order of the adopted quadrature amplitude modulation (QAM) constellation and $\lfloor \cdot \rfloor$ denotes the floor operator. Hence, the subblock spectral efficiency of OFDM-ISNM is given by

$$SE_{\mathrm{ISNM}}^{\mathrm{subblock}} = \frac{b}{n} = \frac{\lfloor \log_2(M^{k_1} + M^{k_2} + \cdots + M^{k_l}) \rfloor}{n}. \tag{2}$$

Obviously, as long as the length of subblock n is confirmed, the spectral efficiency is determined by the adopted K set and M. The mapping table of OFDM-ISNM with $n = 4$, $K = \{0, 1, 2\}$ and $M = 4$, achieving a spectral efficiency of 1 bit/s/Hz is given in Table 1, where S_1, S_2, S_3 and S_4 denote the 4QAM constellation symbols. Consequently, a total of G subblocks are generated. Furthermore, subblock interleaving is employed to mitigate the low-pass effect of the UOWC

Optics EXPRESS

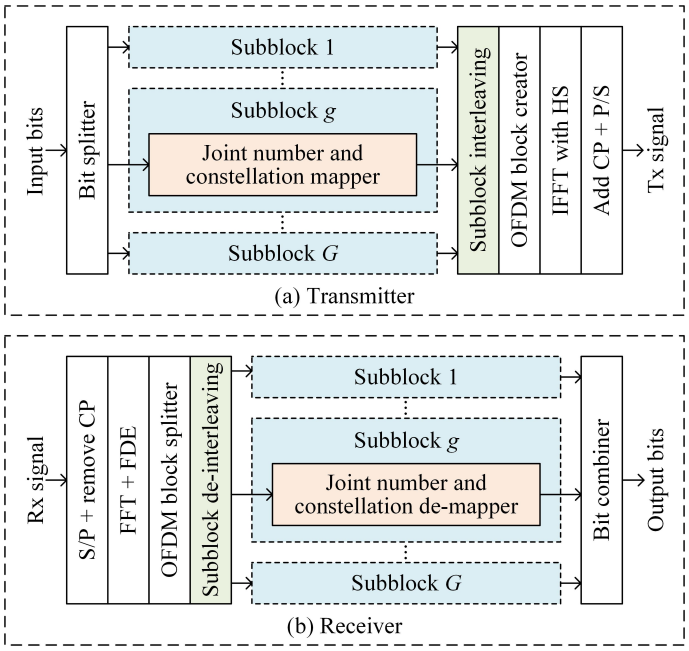

Fig. 1. Principle of OFDM-ISNM: (a) transmitter and (b) receiver.

system. The detailed principle of subblock interleaving will be introduced in Section 2.2. After the concatenation of G subblocks, the whole OFDM block is created. Finally, the transmitted signal is obtained by taking inverse fast Fourier transform (IFFT) with Hermitian symmetry (HS), adding cyclic prefix (CP) and the parallel-to-serial (P/S) conversion.

Table 1. Mapping Table for $n = 4$, $K = \{0, 1, 2\}$ and $M = 4$

Information bits	Number of activated subcarriers	Subblock data
0 0 0 0	0	$[0, 0, 0, 0]$
0 0 0 1	1	$[S_1, 0, 0, 0]$
...	...	...
0 1 0 0	1	$[S_4, 0, 0, 0]$
0 1 0 1	2	$[S_1, S_1, 0, 0]$
0 1 1 0	2	$[S_1, S_2, 0, 0]$
...	...	...
1 1 1 0	2	$[S_3, S_2, 0, 0]$
1 1 1 1	2	$[S_3, S_3, 0, 0]$

According to Eq. (2), the achievable data rate of the bandlimited UOWC system applying OFDM-ISNM can be obtained by

$$R_{\mathrm{ISNM}} = SE_{\mathrm{ISNM}}^{\mathrm{subblock}} B_{\mathrm{effective}}, \tag{3}$$

where $B_{\mathrm{effective}}$ denotes the effective bandwidth of the system, which is defined by

$$B_{\mathrm{effective}} = \frac{N}{N_{\mathrm{IFFT}} + N_{\mathrm{CP}}} R_s, \tag{4}$$

Optics EXPRESS

where N_{IFFT}, N_{CP} and R_s denote the size of IFFT, the size of CP and the sampling rate of the transmitter, respectively.

In the OFDM-ISNM receiver, as can be seen in Fig. 1(b), the received OFDM-ISNM signal undergoes serial-to-parallel (S/P) conversion, removing CP, FFT and frequency-domain equalization (FDE). Afterwards, the OFDM block is split into G subblocks and subblock de-interleaving is then executed. In each subblock, joint number and constellation de-mapping is performed through maximum-likelihood (ML) detection to achieve optimal performance according to the mapping table. Note that the receiver does not need to decide which subcarriers are activated due to the use of ML detection, and hence the error propagation issue can be addressed. Finally, bits from each subblock are combined to obtain the output bits. The complexity of the proposed OFDM-ISNM scheme mainly comes from the ML detection for joint number and constellation de-mapping at the receiver side. For an OFDM-ISNM subblock with length n and achieving a spectral efficiency of λ, the complexity in terms of complex multiplications is $\sim O(2^{\lambda}n)$ per subblock.

2.2. Subblock interleaving

In order to address the low-pass effect of the bandlimited UOWC system, subblock interleaving is proposed and discussed in this subsection. Figures 2(a) and 2(b) illustrate the transmitted OFDM-SNM spectrum without and with subblock interleaving, respectively, by taking $n = 4$ and $k = 2$ as an example. For the case without subblock interleaving, as shown in Fig. 2(a), the subcarriers in the low-frequency region are selected for activation in each subblock and hence the low-pass effect within each subblock can be mitigated. However, the low-pass effect among

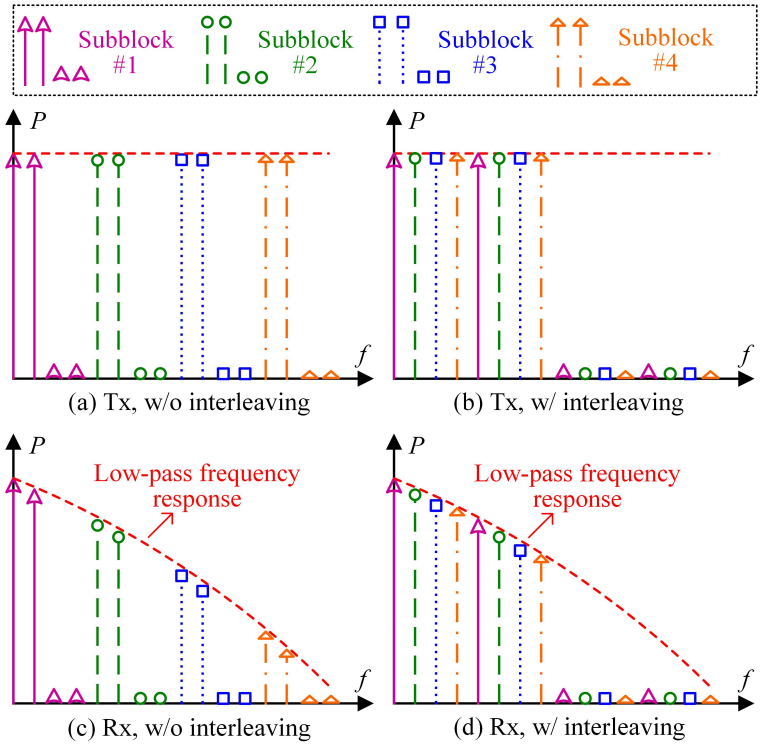

Fig. 2. Illustration of OFDM-SNM spectrum: (a) Tx, w/o interleaving, (b) Tx, w/ interleaving, (c) Rx, w/o interleaving, and (d) Rx, w/ interleaving.

Optics EXPRESS

different subblocks is still a problem, as the activated subcarriers are distributed across the entire frequency band. In contrast, for the case with subblock interleaving as shown in Fig. 2(b), all the activated subcarriers are distributed in the low-frequency region.

Figures 2(c) and 2(d) depict the received OFDM-SNM spectrum without and with interleaving, respectively. As can be seen in Fig. 2(c), the activated subcarriers in the high frequency region suffer from more severe power attenuation, resulting from the low-pass frequency response of the bandlimited UOWC system. Nevertheless, when subblock interleaving is performed, as shown in Fig. 2(d), subcarriers carrying the constellation symbols, i.e., activated subcarriers, are concentrated in the low-frequency region. Consequently, the power attenuation of the activated subcarriers is diminished significantly by employing subblock interleaving. In this current work, a sequential subcarrier placement scheme is adopted to interleave all the activated subcarriers in the low-frequency region, which might not be optimal. The investigation of optimal subcarrier placement for the proposed OFDM-ISNM scheme will be considered in our future work.

3. Results and discussions

In this section, we conduct both simulations and experiments to evaluate the performance of a bandlimited UOWC system applying OFDM-ISNM. Moreover, for the purpose of comparison, plain OFDM, OFDM-SIM, OFDM with interleaved SIM (OFDM-ISIM) and OFDM-SNM are considered as benchmark schemes during the simulation and experimental evaluations.

3.1. Simulation results

In the simulations, we consider a bandlimited UOWC system over an additive white Gaussian noise (AWGN) channel with a low-pass frequency response measured from the experimental UOWC system. The measured low-pass frequency response is plotted in Fig. 3, where the -3dB modulation bandwidth is 0.9 GHz. Moreover, the length of IFFT/FFT, the number of data subcarriers and the size of each subblock in OFDM-ISNM are set to 256, 108 and $n = 4$, respectively. Due to the line-of-sight (LOS) transmission nature of general UOWC systems, the multi-path effect might be negligible and hence no CP is used in OFDM-ISNM.

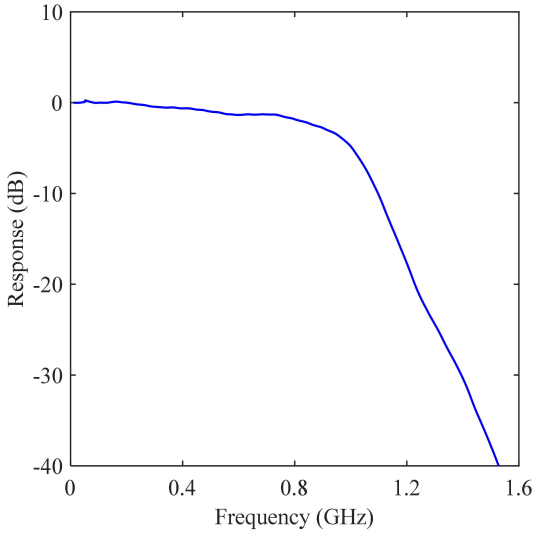

Fig. 3. Measured low-pass frequency response from the experimental UOWC system.

Optics EXPRESS

Figure 4 shows the spectral efficiency versus M for different schemes including plain OFDM, OFDM-SIM and OFDM-SNM. It should be noted that subblock interleaving does not affect the spectral efficiency of the scheme. For OFDM-SIM with a subblock size of n and an activated subcarrier number of k, the spectral efficiency of each subblock in OFDM-SIM is given by [17,18]

$$SE_{\mathrm{SIM}} = \frac{\lfloor(\log_2(C(n,k)))\rfloor + k\log_2(M)}{n}, \tag{5}$$

where $C(\cdot,\cdot)$ denotes the binomial coefficient. As we can see, a larger spectral efficiency is obtained with a larger k value for OFDM-SIM, while a larger spectral efficiency is achieved when a larger k value is included in the K set for OFDM-SNM. Specifically, plain OFDM and OFDM-SNM with $K = \{0, 1, 4\}$ can obtain the same spectral efficiency. Moreover, to achieve the same spectral efficiency for OFDM-SNM, a smaller M can be used when a larger k is adopted. In the following, four different spectral efficiencies (1, 1.5, 2 and 3 bits/s/Hz) are considered for BER performance evaluation and the required modulation orders, i.e. M, can be obtained from Fig. 4 so as to ensure the same target spectral efficiency for all the considered schemes.

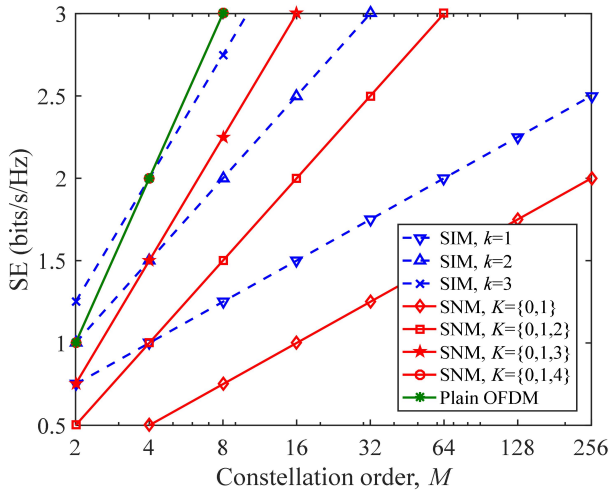

Fig. 4. Spectral efficiency vs. M for different schemes.

Figure 5 depicts the simulation BER versus effective bandwidth for different schemes with different spectral efficiencies. For a spectral efficiency of 1 bit/s/Hz with an SNR of 10 dB, as shown in Fig. 5(a), the maximum usable bandwidths of all the benchmark schemes including plain OFDM, OFDM-SIM, OFDM-ISIM and OFDM-SNM hardly reach 1.3 GHz, considering the 7% forward error correction (FEC) limit of BER = 3.8×10^{-3}. In contrast, the maximum bandwidth that can be used by OFDM-ISNM with $K = \{0, 1, 2\}$ reaches 2.1 GHz, which is corresponding to a capacity improvement of 61.5%. Nevertheless, OFDM-ISNM with both $K = \{0, 1\}$ and $K = \{0, 1, 4\}$ can hardly achieve performance improvements. For a spectral efficiency of 1.5 bits/s/Hz with an SNR of 14 dB, as shown in Fig. 5(b), OFDM-ISNM with $K = \{0, 1, 3\}$ outperforms the benchmark schemes, while OFDM-ISNM with $K = \{0, 1, 2\}$ still obtains the best performance. For higher spectral efficiencies of 2 and 3 bits/s/Hz, the best performance is always achieved by OFDM-ISNM with $K = \{0, 1, 2\}$, when a relatively high SNR is guaranteed.

Figure 6 shows the simulation BER versus SNR for different schemes with different spectral efficiencies, where an effective bandwidth of 1.3 GHz is considered. For a spectral efficiency of 1 bit/s/Hz, as plotted in Fig. 6(a), an SNR of 24.3dB is needed by plain OFDM to reach

Optics EXPRESS

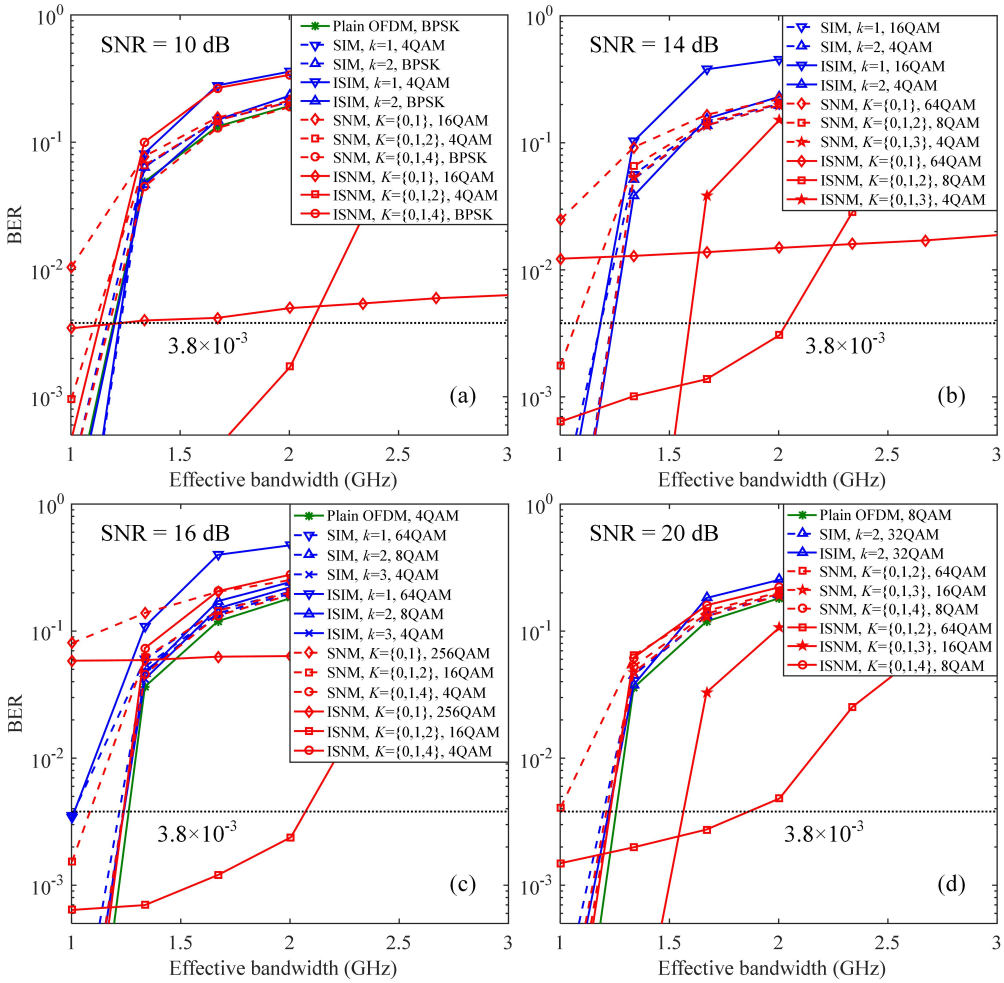

Fig. 5. Simulation BER vs. effective bandwidth for different schemes with a spectral efficiency of (a) 1 bit/s/Hz, (b) 1.5 bits/s/Hz, (c) 2 bits/s/Hz, and (d) 3 bits/s/Hz.

BER = 3.8×10^{-3}, while the OFDM-ISIM schemes require SNRs of about 21 dB to meet the FEC limit. It is exciting to observe that much lower SNRs of 7.6 and 10.1 dB are required by OFDM-ISNM with $K = \{0, 1, 2\}$ and $K = \{0, 1\}$ to reach BER = 3.8×10^{-3}, respectively. As a result, a significant 10.9dB SNR gain is obtained by OFDM-ISNM with $K = \{0, 1\}$ in comparison to the benchmark schemes. Moreover, OFDM-ISNM with $K = \{0, 1, 2\}$ further outperforms OFDM-ISNM with $K = \{0, 1\}$ by an SNR gain of 2.5 dB. When the spectral efficiency is increased, as can be seen from Figs. 6(b)-(d), the best performance is obtained by OFDM-ISNM with $K = \{0, 1, 3\}$ at the spectral efficiencies of 1.5 and 3 bits/s/Hz, while OFDM-ISNM with $K = \{0, 1, 2\}$ also performs the best at the spectral efficiency of 2 bit/s/Hz. It can be concluded from Fig. 6 that the proposed OFDM-ISNM scheme exhibits superior BER performance in bandlimited UOWC systems.

3.2. Experimental results

Figure 7 depicts the experimental setup of a point-to-point UOWC system utilizing a vertical-cavity surface-emitting laser (VCSEL). As can be seen, the transmitted signal generated offline

Optics EXPRESS

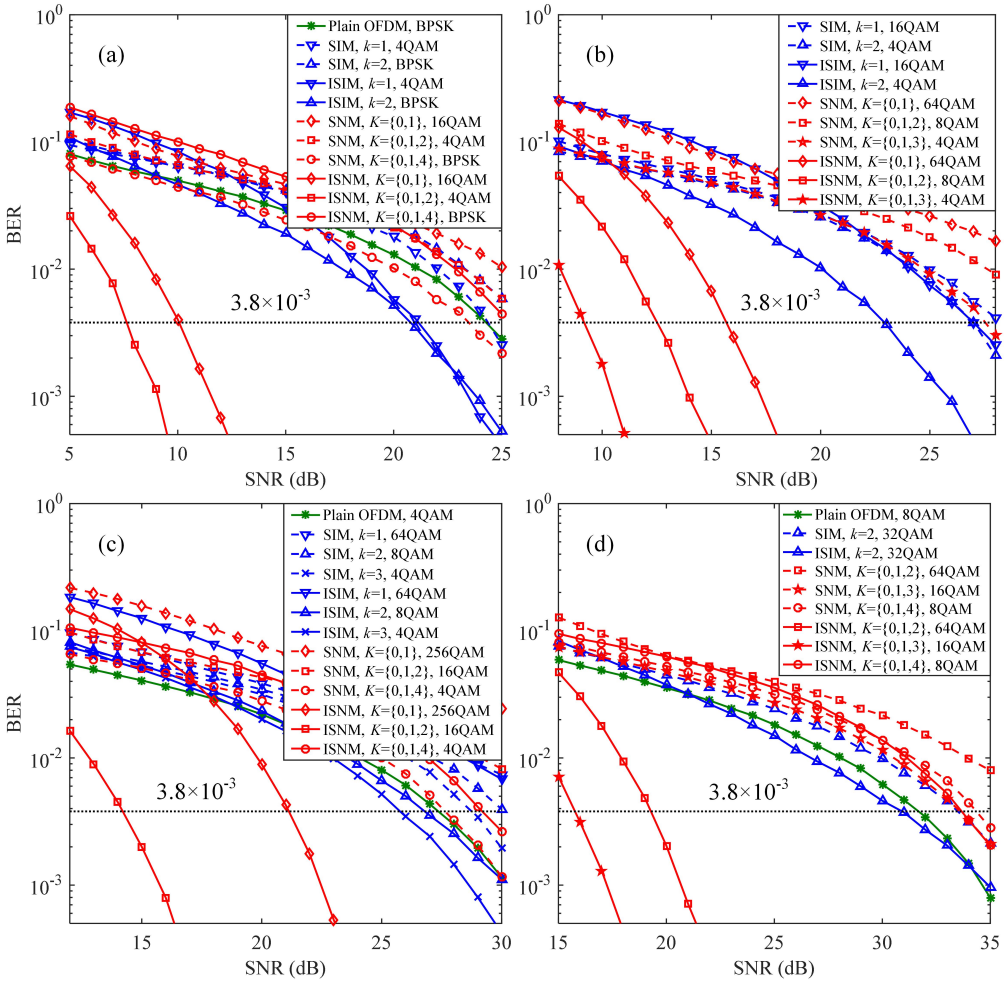

Fig. 6. Simulation BER vs. SNR for different schemes with an effective bandwidth of 1.3 GHz and a spectral efficiency of (a) 1 bit/s/Hz, (b) 1.5 bits/s/Hz, (c) 2 bits/s/Hz, and (d) 3 bits/s/Hz.

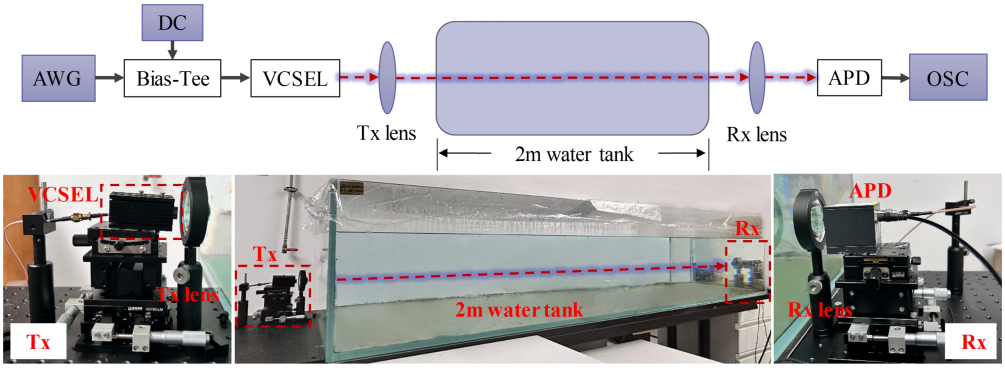

Fig. 7. Experimental setup of the VCSEL-based UOWC system with a 2m water tank.

Optics EXPRESS

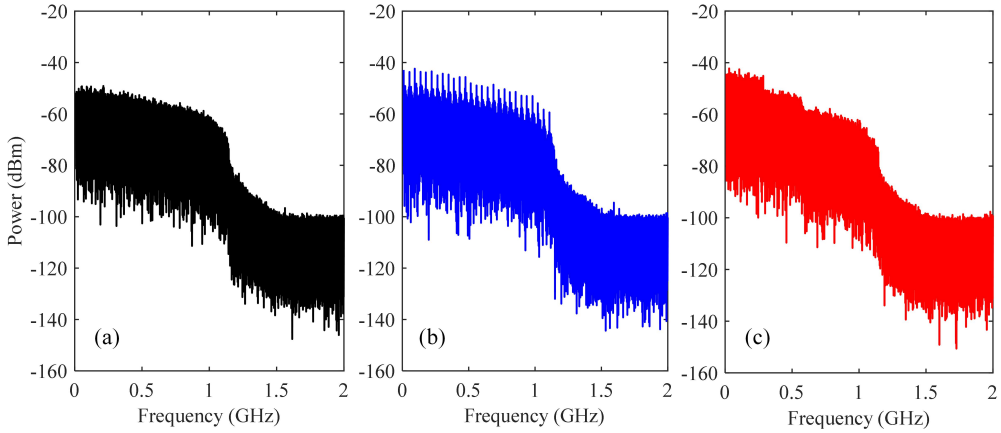

Fig. 8. Received electrical spectrum of (a) plain OFDM, (b) OFDM-SNM with $K = \{0, 1, 2\}$, and (c) OFDM-ISNM with $K = \{0, 1, 2\}$.

by MATLAB is first sent to an arbitrary waveform generator (AWG, Tektronix AWG7101) with a 10-bit vertical solution and a maximum sampling rate of 10 GSa/s. Then, a DC bias current is combined with the AWG output signal via a bias-tee (bias-T, Mini-circuit ZFBT-6GW+) to drive a red VCSEL (DERAY DV0688M). The light emitted by the VCSEL passes through a biconvex lens and propagates through the underwater channel. At the receiver side, another biconvex lens is utilized to focus the light onto the active area of an avalanche photodiode (APD, Menlo Systems APD210) with a bandwidth of about 1 GHz and a frequency range from 1 MHz to 1.6 GHz. After that, the output electrical signal of the APD is recorded by a digital storage oscilloscope (DSO, Tektronix MSO73304DX) with an 8-bit vertical resolution and a fixed sampling rate of 25 GSa/s, and the resultant digital signal is further processed offline by MATLAB. Besides, the frequency response of the whole system is measured by a network analyzer (Keysight N5227A). Moreover, the parameters of OFDM-ISNM are the same as that in the simulations.

Figures 8(a), 8(b) and 8(c) present the received electrical spectrum of plain OFDM, OFDM-SNM with $K = \{0, 1, 2\}$ and OFDM-ISNM with $K = \{0, 1, 2\}$, respectively. For plain OFDM, as shown in Fig. 8(a), the received power of the subcarriers in the high-frequency region has a lower magnitude than that in the low-frequency region, which is resulted from the low-pass effect of the bandlimited UOWC system. For OFDM-SNM with $K = \{0, 1, 2\}$, as shown in Fig. 8(b), the activated subcarriers are distributed across the entire frequency band, which inevitably suffer from the adverse effect of the low-pass characteristic of the bandlimited UOWC system. In contrast, for OFDM-ISNM with $K = \{0, 1, 2\}$, as shown in Fig. 8(c), all of the activated subcarriers are concentrated in the low-frequency region due to the execution of subblock interleaving, and hence the low-pass effect can be efficiently mitigated.

Figure 9 shows the BER versus data rate for different schemes with different spectral efficiencies. For a spectral efficiency of 1 bit/s/Hz, as shown in Fig. 9(a), it is clearly observed that OFDM-ISNM with $K = \{0, 1, 2\}$ performs the best among all the schemes. Moreover, OFDM-ISNM with $K = \{0, 1\}$ can barely reach the FEC limit of BER = 3.8×10^{-3} due to the use of a high-order constellation, while OFDM-ISNM with $K = \{0, 1, 4\}$ also performs much worse than OFDM-ISNM with $K = \{0, 1, 2\}$ due to the severe low-pass effect. Hence, the selection of a proper K set is vital for the proposed OFDM-ISNM scheme to achieve a trade-off between constellation order and low-pass effect. Besides, as we can see, subblock interleaving has nearly no improvement on the BER performance of OFDM-SNM with $K = \{0, 1, 4\}$, which can be attributed to the fact that whether subblock interleaving is performed or not, the activated subcarriers are always distributed over the entire frequency band. Compared with the benchmark OFDM-ISIM schemes,

Optics EXPRESS

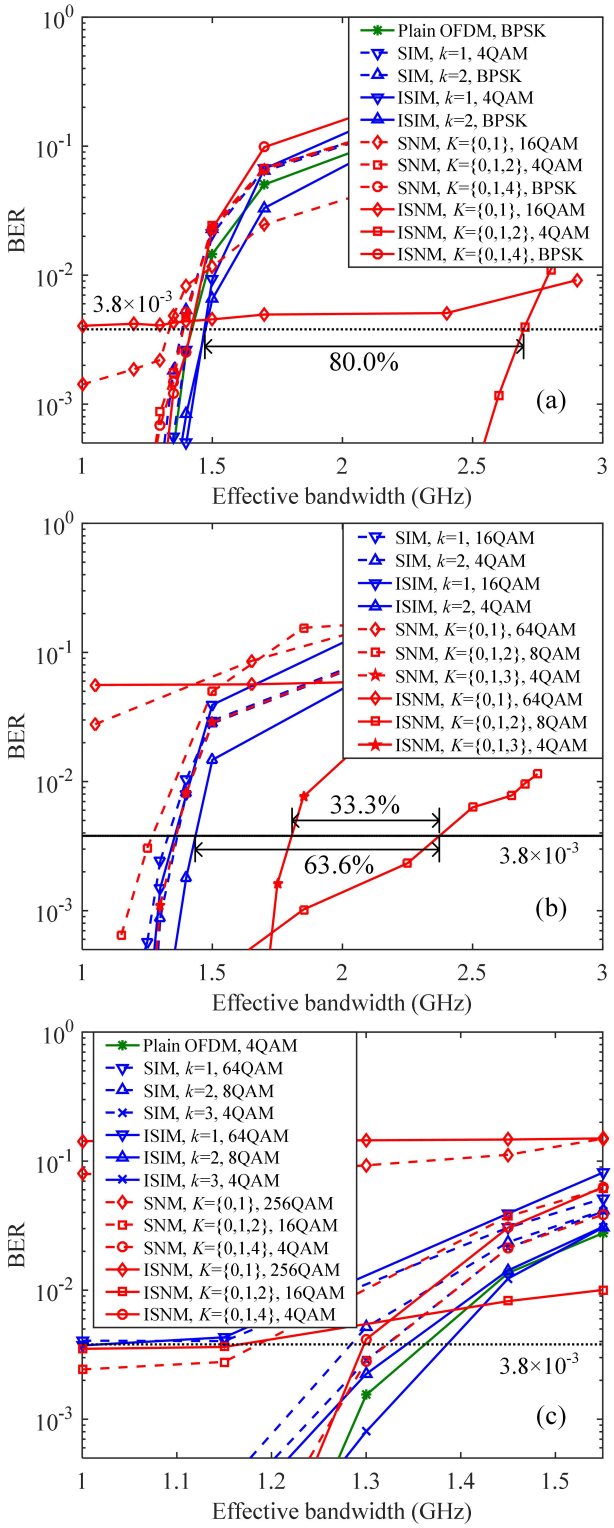

Fig. 9. Experimental BER vs. data rate for different schemes with a spectral efficiency of (a) 1 bit/s/Hz, (b) 1.5 bits/s/Hz, and (c) 2 bits/s/Hz.

Optics EXPRESS

a 80.0% data rate improvement can be obtained by OFDM-ISNM with $K = \{0, 1, 2\}$. For a spectral efficiency of 1.5 bits/s/Hz, as shown in Fig. 9(b), both OFDM-SNM and OFDM-ISNM with $K = \{0, 1\}$ can barely reach the FEC limit, while OFDM-ISNM with $K = \{0, 1, 2\}$ still achieves the best performance. More specifically, OFDM-ISNM with $K = \{0, 1, 2\}$ outperforms OFDM-ISIM with $k = 2$ by a data rate improvement of 63.6%, which also obtains 33.3% data rate improvement over OFDM-ISNM with $K = \{0, 1, 3\}$. For a relatively high spectral efficiency of 2 bits/s/Hz, as shown in Fig. 9(c), it can be seen that the proposed OFDM-ISNM schemes cannot achieve satisfactory performance, which is mainly because the BER performance is dominated by the high-order constellation symbols while the received SNR is relatively low. For even higher spectral efficiencies, all the considered schemes cannot obtain higher data rates due to the limited received SNR.

Finally, we compare the maximum achievable data rates of different schemes with different spectral efficiencies, where the unit of spectral efficiency is bits/s/Hz. Table 2 summarizes the maximum achievable data rates of different schemes under different spectral efficiencies. Taking the spectral efficiency of 1.5 bits/s/Hz as an example, the maximum achievable data rate of OFDM-SIM is 2.0 Gbps, which is obtained with $k = 2$. Moreover, the maximum achievable data rate of OFDM-ISIM is 2.2 Gbps, which is also obtained with $k = 2$. For OFDM-SNM, it performs the best with $K = \{0, 1, 3\}$ and achieves the same maximum data rate as OFDM-SIM with $k = 2$. In contrast, the maximum achievable data rate reaches 3.6 Gbps for OFDM-ISNM with $K = \{0, 1, 2\}$. Compared with OFDM-SNM, a significant 80% achievable data rate improvement can be obtained by OFDM-ISNM at the spectral efficiency of 1.5 bits/s/Hz. Moreover, for all the benchmark schemes at different spectral efficiencies, both plain OFDM and OFDM-ISIM achieve the highest data rate of 2.8 Gbps at the same spectral efficiency of 2 bits/s/Hz. Therefore, in comparison to all the benchmark schemes, OFDM-ISNM achieves a remarkable data rate improvement of 28.6%.

Table 2. Maximum achievable data rates of different schemes

Scheme	Plain OFDM	OFDM-SIM	OFDM-ISIM	OFDM-SNM	OFDM-ISNM
SE = 1	1.4 Gbps	1.4 Gbps	1.5 Gbps	1.4 Gbps	2.7 Gbps
SE = 1.5	/	2.0 Gbps	2.2 Gbps	2.0 Gbps	3.6 Gbps
SE = 2	2.8 Gbps	2.6 Gbps	2.8 Gbps	2.6 Gbps	2.6 Gbps

4. Conclusion

In this paper, we have proposed and evaluated a novel OFDM-ISNM scheme for efficient capacity enhancement in bandlimited UOWC systems. By performing joint number and constellation mapping/de-mapping with subblock interleaving, the activated subcarriers can be concentrated in the low-frequency region and hence the adverse low-pass effect of the bandlimited UOWC system can be mitigated. Experimental results show that there exists a trade-off between the adopted K set and M, and a proper selection of K set and M can efficiently improve the achievable data rate of the bandlimited UOWC system. It is demonstrated by the experimental results that OFDM-ISNM can obtain a remarkable 28.6% data rate improvement compared with all the considered benchmark schemes. Therefore, the proposed OFDM-ISNM scheme can be a promising candidate for practical bandlimited UOWC systems.

Funding. National Natural Science Foundation of China (62271091, 61901065); Natural Science Foundation of Chongqing (cstc2021jcyj-msxmX0480).

Disclosures. The authors declare no conflicts of interest.

Data availability. The data underlying the results presented in this paper are not publicly available at this time but may be obtained from the authors upon reasonable request.

Optics EXPRESS

References

1. S. Arnon, "Underwater optical wireless communication network," Opt. Eng. **49**(1), 015001 (2010).
2. Z. Zeng, S. Fu, H. Zhang, Y. Dong, and J. Cheng, "A survey of underwater optical wireless communications," IEEE Commun. Surv. Tuts. **19**(1), 204–238 (2017).
3. G. Cossu, R. Corsini, A. Khalid, S. Balestrino, A. Coppelli, A. Caiti, and E. Ciaramella, "Experimental demonstration of high speed underwater visible light communications," in *Proc. IEEE Int. Workshops Opt. Wireless Commun. (IWOW)*, (2013), pp. 11–15.
4. M. Elamassie, F. Miramirkhani, and M. Uysal, "Performance characterization of underwater visible light communication," IEEE Trans. Commun. **67**(1), 543–552 (2019).
5. L. Zhang, Z. Wang, Z. Wei, C. Chen, G. Wei, H. Fu, and Y. Dong, "Towards a 20 Gbps multi-user bubble turbulent NOMA UOWC system with green and blue polarization multiplexing," Opt. Express **28**(21), 31796–31807 (2020).
6. B. Zhuang, C. Li, N. Wu, and Z. Xu, "First demonstration of 400Mb/s PAM4 signal transmission over 10-meter underwater channel using a blue LED and a digital linear pre-equalizer," in *Conference on Lasers and Electro-Optics (CLEO)*, (2017), p. STh3O.3.
7. Y. Zhao and N. Chi, "Partial pruning strategy for a dual-branch multilayer perceptron-based post-equalizer in underwater visible light communication systems," Opt. Express **28**(10), 15562–15572 (2020).
8. C. Fei, R. Chen, J. Du, Y. Wang, J. Tian, G. Zhang, J. Zhang, X. Hong, and S. He, "Underwater wireless optical communication utilizing low-complexity sparse pruned-term-based nonlinear decision-feedback equalization," Appl. Opt. **61**(22), 6534–6543 (2022).
9. J. Shi, W. Niu, Z. Li, C. Shen, J. Zhang, S. Yu, and N. Chi, "Optimal adaptive waveform design utilizing an end-to-end learning-based pre-equalization neural network in an UVLC system," J. Lightwave Technol. **41**(6), 1626–1636 (2023).
10. C. Chen, Y. Nie, M. Liu, Y. Du, R. Liu, Z. Wei, H. Fu, and B. Zhu, "Digital pre-equalization for OFDM-based VLC systems: Centralized or distributed," IEEE Photonics Technol. Lett. **33**(19), 1081–1084 (2021).
11. Y. Song, W. Lu, B. Sun, Y. Hong, F. Qu, J. Han, W. Zhang, and J. Xu, "Experimental demonstration of MIMO-OFDM underwater wireless optical communication," Opt. Commun. **403**, 205–210 (2017).
12. S. Hessien, S. C. Tokgöz, N. Anous, A. Boyacı, M. Abdallah, and K. A. Qaraqe, "Experimental evaluation of OFDM-based underwater visible light communication system," IEEE Photonics J. **10**(5), 1–13 (2018).
13. H. Jiang, H. Qiu, N. He, W. Popoola, Z. Ahmad, and S. Rajbhandari, "Performance of spatial diversity DCO-OFDM in a weak turbulence underwater visible light communication channel," J. Lightwave Technol. **38**(8), 2271–2277 (2020).
14. R. Chen, J. Du, Y. Wang, C. Fei, T. Zhang, J. Tian, G. Zhang, X. Hong, and S. He, "Experimental demonstration of real-time optical DFT-S DMT signal transmission for a blue-LED-based UWOC system using spatial diversity reception," Appl. Opt. **62**(3), 541–551 (2023).
15. C. T. Geldard and W. O. Popoola, "Experimental comparison of modulation techniques for led-based underwater optical wireless communications," in *IEEE Wireless Communications and Networking Conference (WCNC)*, (IEEE, 2023), pp. 1–6.
16. X. Jin, J. Wei, R. Giddings, T. Quinlan, S. Walker, and J. Tang, "Experimental demonstrations and extensive comparisons of end-to-end real-time optical OFDM transceivers with adaptive bit and/or power loading," IEEE Photonics J. **3**(3), 500–511 (2011).
17. E. Başar and E. Panayırcı, "Optical OFDM with index modulation for visible light communications," in *IEEE Int. Workshops Opt. Wireless Commun. (IWOW)*, (2015), pp. 11–15.
18. F. Ahmed, Y. Nie, C. Chen, M. Liu, P. Du, and A. Alphones, "DFT-spread OFDM with quadrature index modulation for practical VLC systems," Opt. Express **29**(21), 33027–33036 (2021).
19. C. Chen, Y. Nie, F. Ahmed, Z. Zeng, and M. Liu, "Constellation design of DFT-S-OFDM with dual-mode index modulation in VLC," Opt. Express **30**(16), 28371–28384 (2022).
20. Z. A. Qasem, A. Ali, B. Deng, Q. Li, and H. Fu, "Unipolar X-transform OFDM with index modulation for underwater optical wireless communications," IEEE Photonics Technol. Lett. **35**(11), 581–584 (2023).
21. A. M. Jaradat, J. M. Hamamreh, and H. Arslan, "OFDM with subcarrier number modulation," IEEE Wirel. Commun. Lett. **7**(6), 914–917 (2018).
22. M. Wen, J. Li, S. Dang, Q. Li, S. Mumtaz, and H. Arslan, "Joint-mapping orthogonal frequency division multiplexing with subcarrier number modulation," IEEE Trans. Commun. **69**(7), 4306–4318 (2021).